Magnetic states in frustrated bilayer models: The ordered phase of mixed-layer pnictide oxides

Matthew Enjalran
Department of Physics, University of California, Davis, California 95616
and Materials Research Institute, Lawrence Livermore National Laboratory, University of California, Livermore, California 94550

Richard T. Scalettar
Department of Physics, University of California, Davis, California 95616

Susan M. Kauzlarich
Department of Chemistry, University of California, Davis, California 95616

(Received 3 January 2000)

We present results from a numerical investigation of bilayer classical spin systems with local interactions and frustration caused by lattice geometry. We find that when two identical square planes are displaced by half a lattice constant in one direction, a transition to a uniformly twisted spin state occurs at $J/J_\perp \geqslant 0.25$. An orthogonal state between layers is obtained in the limit $T=0$ and $J_\perp = 0$. If instead the two layers are offset along a diagonal, we obtain the phase diagram of the classical $J_1 - J_2$ model. A weakly canted phase is observed at the classical transition point of $J/J_\perp = 0.5$, but frustration does not drive the system towards a state of orthogonal interlayer order. We propose a simple bilayer model with two inequivalent square lattices to study the frustrating interactions of the mixed layer pnictide oxides ($Sr_2Mn_3Pn_2O_2$, Pn=As,Sb). We find a ground state composed of two independent Néel ordered layers when the interlayer exchange is an order of magnitude weaker than the intralayer exchange, as suggested by experiment. Evidence for local orthogonal order between the layers is found, but it occurs in regions of parameter space which are not experimentally realized.

I. INTRODUCTION

Models of clean systems of interacting moments have been studied extensively by analytic and numerical techniques, and the ordered phases of models like Ising, Heisenberg, or Hubbard have been determined in various regions of parameter space, with the results having contributed enormously to our understanding of magnetic phenomena and the physics of correlated systems in general.[1] However, real materials are rarely, or never, clean. There is often frustration due to competing interactions and disorder in the interaction strengths. The study of such Hamiltonians is a very active field in physics and material science. Research on spin glasses, magnetic systems with random and frustrated interactions, has been conducted for years; the physics that has been obtained from these magnetic systems is now being applied to the study of related complex phenomena.[2,3]

The work we undertake concerns insulating magnetic systems with frustration but no randomness. Competing interactions that cause magnetic frustration can have many origins, but our focus will be on model systems in which the lattice geometry is the source. In three dimensions, helical magnetic order is observed when geometric frustration is accompanied by anisotropy.[4,5] It has also been suggested that some noncollinear spin-ordered structures belong to a new chiral universality class.[6] However, the model Hamiltonians we study are essentially two dimensional with no anisotropic terms, and our emphasis will be on the nature of the local rather than the long-range magnetic order. Our investigation will employ standard Monte Carlo methods and simple analytic techniques.

The motivation for this work has as its foundation the experimental results of Brock *et al.* for the mixed layer pnictide oxides.[7] A primary focus of their work is the relation of chemistry and structure to the electronic and magnetic properties of compounds such as $Sr_2Mn_3Pn_2O_2$(Pn=As,Sb), where two distinct square geometries of manganese exist in a lattice of space-group symmetry $I4/mmm$. In one layer, manganese is bonded to oxygen in a planar CuO_2 arrangement, MnO_2^{2-}. In a second layer, it is bonded to a pnictogen in a tetrahedral structure, $MnPn_2^{2-}$, where pnictogen atoms project alternately above and below the plane defined by the manganese atoms. From here on we denote the two manganese layers as Mn(1) for MnO_2^{2-} and Mn(2) for $MnPn_2^{2-}$. The manganese atoms carry a spin $S=5/2$.

The magnetic structure of $Sr_2Mn_3Sb_2O_2$, as determined by neutron powder diffraction, is shown in Fig. 1, and is predominantly two dimensional 2D in character. Measurements of the bulk susceptibility support this 2D picture.[7] The Mn(1) substructure is identical to the magnetic structure of K_2NiF_4.[8] Antiferromagnetic order in the respective layers is expected for manganese coupled via superexchange, with a direct exchange contribution possible in the Mn(2) layer.[7] Although the alignment of moments in different layers along orthogonal directions has been observed,[9,10] it could not be explained by simple models initially used to gain insight into the experiments. Specifically, the different temperatures at which the two layers order provide an indication of the relative strengths of the intralayer couplings, 300–340 K for Mn(2) and 50–100 K for Mn(1), with the nearest-neighbor interlayer coupling expected to be weaker by an order of magnitude or more. Once the Mn(2) layer orders, on sym-

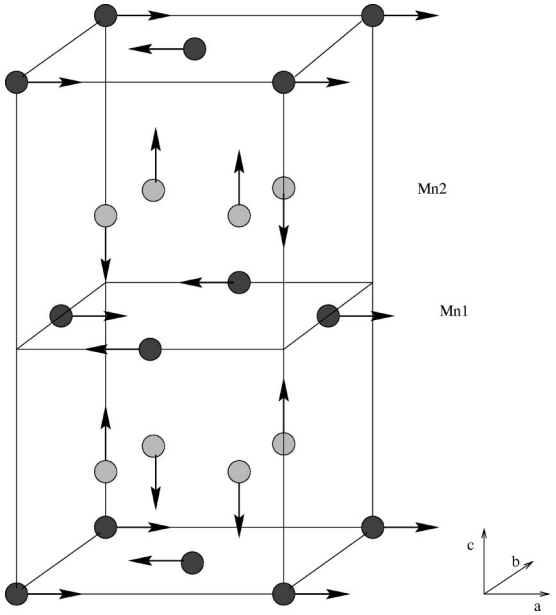

FIG. 1. The proposed magnetic unit cell and ground state of $Sr_2Mn_3Sb_2O_2$. The Mn(1) layers have a square-planar structure; the manganese atoms in the Mn(2) layers also form a square lattice, but the pnictogen atoms (not shown) project alternately above and below the plane. The manganese carry spin $S=5/2$. The structurally distinct layers order at very different temperatures, $T_{\mathrm{Mn(1)}}=50-100$ K and $T_{\mathrm{Mn(2)}}=300-340$ K, and along orthogonal directions.

metry grounds, the spins in the Mn(1) layer should feel a net field of zero from the neighboring planes since the neighboring spins are antiparallel. A Néel ordered Mn(1) layer with a random relative orientation might then at first be expected. However, work by Henley shows this argument is too simplistic. On the frustrated XY model on a square lattice thermal fluctuations can lift the continuous symmetry of the classical Néel state and select a ground state of two collinear Néel ordered sublattices.[11] In the spin$-1/2$ J_1-J_2 model, it is the zero-point fluctuations of the spin waves that select the collinear state.[12] Thus frustrated systems can exhibit order by this nontrivial mechanism. The suggestion for a bilayer system is, therefore, two collinear Néel ordered planes.

Nevertheless, the pnictide oxides remain a puzzle. Since the frustrated interplanar interactions do not favor orthogonal interlayer order in any obvious way, the central issue is the origin of this interlayer magnetic order. It was originally suggested that various magnetic anisotropies could drive the observed interlayer spin patterns. In 2D Heisenberg model systems, it is known that weak anisotropy can induce a phase transition at comparably low temperatures.[13,14] However, there is no experimental evidence for any such anisotropies in the pnictide oxides. It is the purpose of this work to establish that frustration due to nearest-neighbor interactions alone can sometimes yield orthogonal order.

While we focus on two specific transition-metal pnictide oxides, there has been much recent experimental interest in layered magnetic materials. There is a general interest in the synthesis and characterization of layered manganese pnictide oxides,[15,16] and a mixed layered chalcogenide oxide compound has been prepared and studied.[17] Finding an analog to the copper oxides[18] and the study of unusual magnetic and electronic properties[19] are also important motivations for research on layered compounds.

The outline for the remainder of this paper is as follows: In Sec. II we present two frustrated bilayer systems with generic coupling schemes, and the analytic solution to the ground state of each model is discussed. We then discuss the Monte Carlo method used to study these models and present results from our simulations, which extend the analytic results to finite temperatures. We establish that orthogonal interlayer order can arise from interlayer frustration without appealing to spatial anisotropies. Section III is the focus of our study. It begins with a description of a relevant bilayer model for the pnictide oxides. Results from simulations are presented and discussed in terms of the experimental findings. The paper closes with conclusions in Sec. IV.

II. GENERIC BILAYER MODELS

Consider a magnetic system formed from two planes, where a spin on each site is allowed to interact with all its neighbors, intraplanar, and interplanar. A general Hamiltonian can be written as

$$H=\sum_{\alpha} J_{\alpha}\sum_{\langle i,j\rangle}\vec{S}_i^{\alpha}\cdot\vec{S}_j^{\alpha}+J_{\perp}\sum_{\langle i,j\rangle}\vec{S}_i^{\alpha}\cdot\vec{S}_j^{\beta}. \tag{1}$$

We denote the intralayer couplings by J_{α} and the interlayer coupling by $J_{\perp}$. Our focus will be on classical spin systems; hence $\vec{S}_i^{\alpha}$ represents a unit vector at site i in layer α with $|\vec{S}|=(S_x^2+S_y^2+S_z^2)^{1/2}=1$. The relatively large spin-5/2 of the Mn atoms in the pnictide oxides makes this a reasonable approximation. In this section we restrict our study to systems composed of identical square lattices with antiferromagnetic interactions, i.e., $J_1=J_2=J$ with $J>0$ and $J_{\perp}>0$. We note, however, that for bipartite geometries, i.e., those in which the lattice can be divided into two sublattices such that the interacting spins i,j in the Hamiltonian always belong to different sublattices, the sign of J is irrelevant. A simple sublattice rotation changes the sign of J and maps the ferromagnet into the antiferromagnet without any change in the underlying critical behavior beyond that implied by the rotation. The geometry in which the two stacked layers sit directly atop each other is a bipartite situation. In particular, frustration is not present for such geometries.

However, frustration is introduced in the model through staggered geometries or lattice mismatch, which destroy the bipartite structure, and then the sign of $J_{\perp}$ is relevant. One simple frustrated model can be obtained by displacement of the top layer of the stacked system by half a lattice constant along a single lattice direction, e.g., $\hat{y}$. All sites in a plane sit directly above or below the midpoint of a bond in the adjacent plane. The lattice is shown as (i) in Fig. 2. Frustration is present because of the triangular arrangement between spins in different layers. We will refer to this geometry as the zigzag lattice. A 1D version of this model with a single line in the $\hat{y}$ direction has been previously considered. A solvable model for this spin-1/2 zigzag chain shows a dimer state at $J/J_{\perp}=0.5$.[20] However, recent numerical results indicate dimer order for $0.25<J/J_{\perp}<0.5$ and an incommensurate spiral order for $J/J_{\perp}>0.5$.[21]

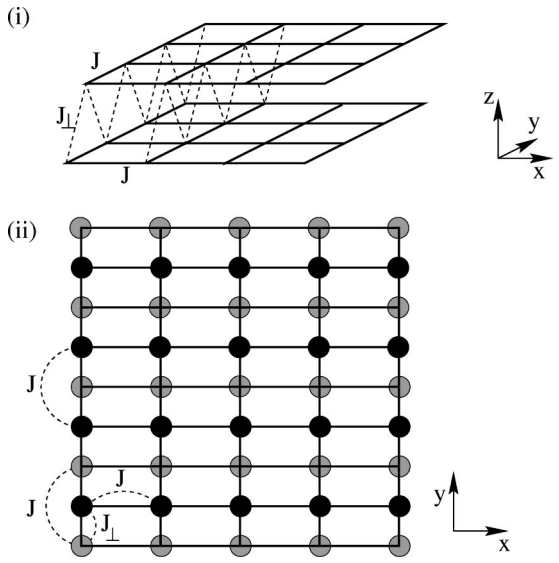

FIG. 2. The zigzag lattice and its 2D projection. In the zigzag lattice, (i), the top square layer is offset from perfect alignment by half a lattice constant in the $\hat{y}$ direction. The two layers are equivalent, and the lattice is frustrated because of the triangular arrangement between spins in different layers. (ii) The zigzag lattice projected on to a plane yields a network of linear chains with first $J_\perp$ and second J neighbor interactions that are antiferromagnetically coupled with interaction strength J. The light and dark circles represent spins from the bottom and top layer, respectively.

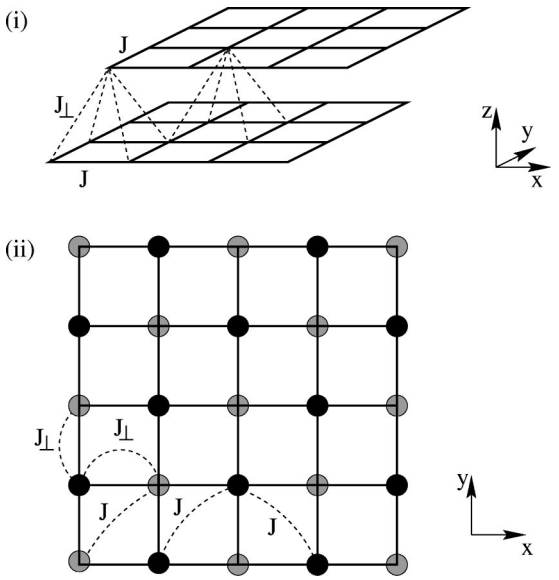

FIG. 3. The diagonal lattice and its 2D projection. (i) The diagonal lattice is obtained by shifting the top layer of the zigzag lattice by half a lattice constant in the $\hat{x}$ direction. The two layers are equivalent and frustration is caused by the triangular geometry between spins in the different layers. (ii) The projection on to a plane yields a square lattice with first $J_\perp$ and second J neighbor interactions. The two layers in (i) correspond to different sublattices here, where the light and dark circles represent spins from the bottom and top layer, respectively.

A second frustrated model is generated by a relative displacement of the top layer of the zigzag lattice by half a lattice constant in the perpendicular direction, $\hat{x}$. The resultant lattice is shown as (i) in Fig. 3. Every site is situated either above or below the center of a square plaquette of spins in the adjacent layer. As in zigzag lattice a triangular arrangement between spins in different layers ensures that the system is frustrated. We will refer to this system as the diagonal lattice. As we shall see, it is equivalent to the planar J_1-J_2 classical Heisenberg model.

A. The ground state

As for most nonrandom classical spin systems (but not quantum-mechanical ones) we can solve for the ground state of the translationally invariant zigzag and diagonal lattices exactly. The standard approach is to form the Fourier transform of the exchange integral, $J(\vec{q})=\Sigma_{\vec{r}}J(\vec{r})e^{i\vec{q}\cdot\vec{r}}$, and then minimize to find the momenta of the stable phases.[4] To simplify the process we map the two bilayer models onto their planar equivalents. These are displayed as (ii) in Figs. 2 and 3. In each case, the phase diagram for the planar model is discussed first, followed by a mapping back to the bilayer system.

In the planar version of the zigzag lattice, where the zigzag structure runs along the $\hat{y}$ direction, the momentum-dependent exchange is given by $J(\vec{q})=2J_\perp\cos q_y+2J\cos 2q_y+2J\cos q_x$. Minimization of $J(\vec{q})$ yields the expressions $2J\sin q_x=0$ and $2J_\perp+8J\cos q_y=0$, from which we obtain the following phase diagram. (i) For antiferromagnetic interactions, one has a classical Néel ordered lattice for $J\leqslant J_\perp/4$, (π,π) order. (ii) When $J>J_\perp/4$, one has incommensurate order along the $\hat{y}$ direction, the direction of frustration. The order is described as (π,q), where q is the uniform twist along the chain of magnitude $\cos q=-J_\perp/4J$. Note that $q=\pi/2$ is obtained in the limit $J_\perp=0$. These results agree with previous findings for the classical zigzag chain.[21] That is, the direction orthogonal to the displacement $(\hat{x})$ is trivial, and the magnetic order simply is a repetition of a set of zigzag chains.

In translating the above conclusions to the bilayer model, it is important to observe that the modulation along the $\hat{x}$ direction remains invariant while the order along the $\hat{y}$ direction changes by a factor of 2. Hence the Néel phase above corresponds to layers with $(\pi,2\pi)$ order, where both the magnetization and staggered magnetization are zero. An accurate picture is one where each layer consists of two Néel ordered sublattices with a π phase shift between the layers. In the incommensurate region of the phase diagram, the order within a layer is $(\pi,2q)$. The uniform twist q is now interpreted as the rotation between nearest-neighbor spins in different layers as one moves along the direction of the zigzag chain. In the limit $q=\pi/2$ a state of orthogonal order between the layers is realized.

As mentioned above, the diagonal lattice can be mapped onto a square lattice with first and second neighbor couplings to yield the classical J_1-J_2 model, where sublattices correspond to layers. We enforce the connection to the bilayer model by relabeling the interactions $J_1=J_\perp$ and $J_2=J_\alpha=J$. Hence the first- and second-neighbor couplings of the planar model are equivalent to the interlayer and intralayer couplings of the bilayer model, respectively. The momentum-dependent exchange integral is now $J(\vec{q})=2J_\perp(\cos q_x$

$+\cos q_y)+4J\cos q_x \cos q_y$, and yields the following phases: (*i*) For antiferromagnetic interactions, minimization of $J(\vec{q})$ reveals a classical Néel state, (π,π) order, for $J<J_\perp/2$. (*ii*) When $J>J_\perp/2$, the stable phase consists of two Néel ordered sublattices, i.e., $(\pi,0)$ order. The two sublattices are independent, so the state is highly degenerate. (*iii*) On the transition line there exists an incommensurate state with a uniform twist between neighbor spins. We find two equivalent states with (π,q) and (q,π) modulation, which are energetically the same as (q,q). In the quantum version of this model, the nature of the transition at $J/J_\perp \gtrsim 0.50$ is an open question.[22,23]

We now map the above results to the diagonal lattice. The (π,π) state of the planar model corresponds to two ferromagnetic layers with opposite magnetization, i.e., there is a π phase shift between the magnetizations. The phase with two Néel ordered sublattices, $(\pi,0)$ or $(0,\pi)$ order, corresponds to two independent Néel ordered layers. On the transition line, $J=J_\perp/2$, the two layers are decoupled and in some incommensurate and highly degenerate state, possibly with (q,q') order.

The important conclusion for analyzing experimental systems like the pnictide oxides is the following: interlayer frustration can apparently result in orthogonal interlayer spin order in certain situations. Specifically, for the zigzag lattice with small $J_\perp$, spins in the two layers are perpendicularly ordered at $T=0$. Therefore, orthogonal order by itself cannot be used as a proof of the presence of magnetic anisotropies.

B. Monte Carlo simulations

We employ the standard Metropolis algorithm[24] for continuous spin systems of moderate size, up to $40\times40\times2=3200$ spins. To satisfy our concern about proper sampling of phase space in the presence of frustration, where rough energy landscapes are a potential problem, fixed temperature simulations in each region of the respective phase diagrams were performed with random, Néel, and ferromagnetic initial configurations in the layers. In all cases considered, convergence to a unique solution was observed. Our results also compare well to the analytic solutions at $T=0$. Monte Carlo data presented are from runs with random initial spin configurations.

To distinguish between the different phases within each model system, we measured several observables. The ground-state energy per spin, $E=\langle H\rangle/N$, has an analytic form for each model and thus can be used for comparison purposes. To probe the local magnetic order, both intralayer and interlayer, we defined a pair of local spin-spin correlation functions that distinguish between parallel and perpendicular orientations,

$$C_\parallel^{\alpha,\beta}=\left\langle \frac{1}{zN_\alpha}\sum_i \sum_{\vec{\delta}} (\vec{S}_i^{\alpha}\cdot\vec{S}_{i+\vec{\delta}}^{\beta})^2 \right\rangle, \tag{2}$$

and

$$C_\perp^{\alpha,\beta}=\left\langle \frac{1}{zN_\alpha}\sum_i \sum_{\vec{\delta}} (\vec{S}_i^{\alpha}\times\vec{S}_{i+\vec{\delta}}^{\beta})^2 \right\rangle. \tag{3}$$

We refer to these as the collinear, $C_\parallel^{\alpha,\beta}$, and perpendicular, $C_\perp^{\alpha,\beta}$, correlation functions. Superscripts $(\alpha,\beta=1,2)$ label the layers, hence $\alpha=\beta$ represents intralayer correlations while $\alpha\neq\beta$ represents interlayer correlations. The sum in i is over all sites in a given layer and the sum over $\vec{\delta}$ involves the nearest-neighbor interactions to site i along the $\hat{x}$ and $\hat{y}$ directions. The factor N_α represents the number of sites in layer α and z is the coordination number. For classical spins, $C_\parallel$ and $C_\perp$ measure the averages $\langle\cos^2\theta\rangle$ and $\langle\sin^2\theta\rangle$, where θ is the angle between nearest-neighbor spins, and hence $C_\parallel$ is large for parallel spins $(\theta=0,\pi)$ and small for perpendicular ones $(\theta=\pi/2)$. In addition, their sum is always unity. In the high-temperature limit, e.g., paramagnetic phase, these functions approach the values $C_\parallel\to1/3$ and $C_\perp\to2/3$, respectively.

While our primary interest is in a local ordering phenomenon—Do adjacent spins in different layers preferentially orient in orthogonal directions or not?—we also measure quantities that tell us about the presence of long-range correlations in our model systems. Therefore, we measured the root-mean-square magnetization

$$M^\alpha=\sqrt{\langle(M_x^\alpha)^2\rangle+\langle(M_y^\alpha)^2\rangle+\langle(M_z^\alpha)^2\rangle}, \tag{4}$$

where

$$(M_a^\alpha)^2=\left(\frac{1}{N_\alpha}\sum_{i\in\alpha} S_{i,a}^\alpha\right)^2,$$

and root-mean-square staggered magnetization

$$M_s^\alpha=\sqrt{\langle(M_{sx}^\alpha)^2\rangle+\langle(M_{sy}^\alpha)^2\rangle+\langle(M_{sz}^\alpha)^2\rangle}, \tag{5}$$

where

$$(M_{sa}^\alpha)^2=\left[\frac{1}{N_\alpha}\left(\sum_{i\in\alpha} S_{i,a}^\alpha-\sum_{j\in\alpha} S_{j,a}^\alpha\right)\right]^2,$$

of each layer. The 2D classical Heisenberg model has long-range order only at $T=0$, and we do not expect these bilayer models to behave any differently. However, the correlation length ξ rises very rapidly as T is lowered. When it eclipses our sample size, we have maximum values for M^α or M_s^α, i.e., $M^\alpha=M_s^\alpha=1.0$.

We begin with the zigzag lattice. We performed simulations on systems of linear size $n=40$, or 3200 spins, with open boundary conditions. Periodic boundary conditions can interfere with the system's preferred order if nq is not a multiple of 2π. Edge effects were not appreciable beyond the perimeter sites. Hence averages were formed from all sites except those in the outer strip of the lattice. For each value of $J/J_\perp$, where $J_\perp=1.0$, the lattice was equilibrated for 15 000 sweeps and then 15 000 measurements of our observables were made. One sweep represents one update of all spins in the system. The interval between measurements varied with temperature and coupling strength, the range being from 10 to 40. Error bars represent the standard deviation of the observable. Note that we used $k_B=1$ in all simulations.

In setting the interaction strengths to $J/J_\perp=0.15$, 0.25, 1.0, 5.0 and sweeping through temperature, we were able to capture the temperature evolution of the three phases of interest. In the (π,π) region of the phase diagram, $J/J_\perp=0.15$, and at the transition point, $J/J_\perp=0.25$, we found that for $T<J_\perp$ a collinear state between

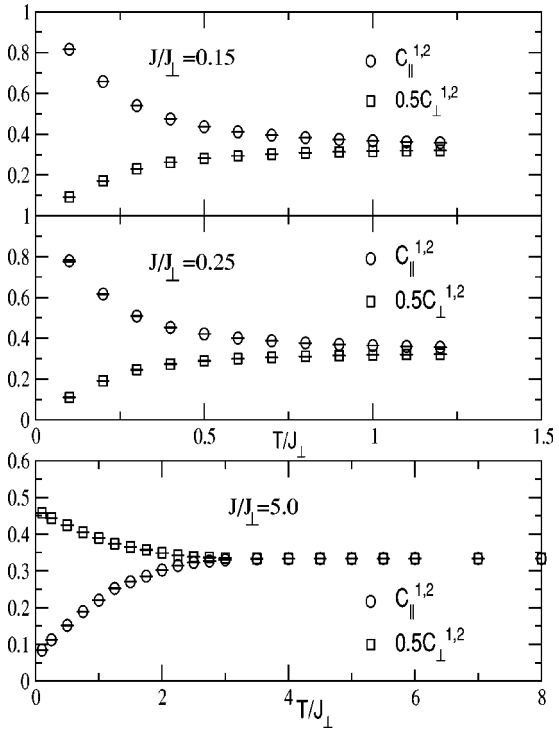

FIG. 4. Temperature dependence of the local interlayer spin-spin correlation functions for the zigzag lattice. $C_{\parallel}^{1,2}$ and $0.5C_{\perp}^{1,2}$ are plotted so that both give 1/3 in the high-temperature limit. At $J/J_{\perp}=0.15$ a collinear state is observed at low temperatures. The collinear state is still present at the transition point, $J/J_{\perp}=0.25$, but for larger values a uniformly twisted spin state is expected. The presence of the twisted state is indicated by an enhanced perpendicular correlation at low temperatures, which is clearly shown for the case of $J/J_{\perp}=5.0$.

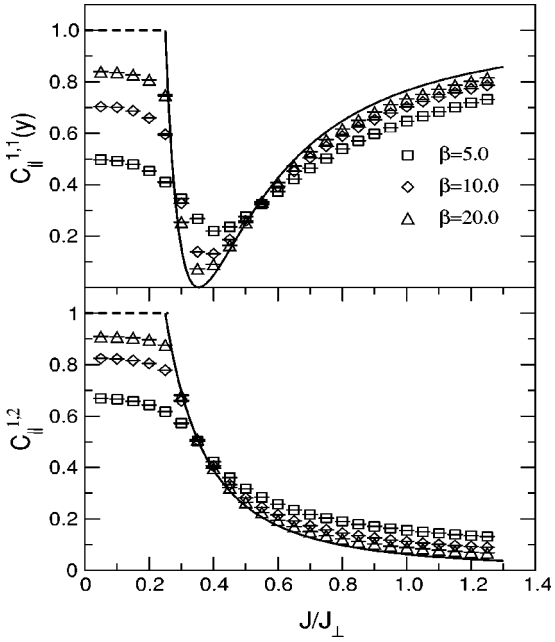

FIG. 5. The spin-spin correlations as a function of interaction strength for the zigzag lattice. In the bottom panel the interlayer collinear correlation shows increasing parallel alignment between the layers as the inverse temperature is increased for $J/J_{\perp}\leqslant 0.25$. The dashed line is the $T=0$ analytic result. Above this transition point, the uniformly twisted spin state is established. Convergence to the $T=0$ analytic solution (solid line) improves with increasing β. An orthogonal state, $C_{\parallel}^{1,2}\rightarrow 0$, is obtained in the thermodynamic limit. In the top panel, the intralayer collinear correlation along the direction of frustration $\hat{y}$ also shows convergence to the $T=0$ analytic solutions (dashed and solid lines) with increasing β.

nearest-neighbor spins in different layers was favored. This was signaled by an enhancement of the interlayer collinear correlation, $C_{\parallel}^{1,2}$, relative to the high-temperature limit of 1/3 at low T. The layers showed no net magnetization. Moving the simulation into the twisted spin region of the phase diagram, $J/J_{\perp}=1.0,\ 5.0$, we observed an enhancement in the perpendicular interlayer correlation, $C_{\perp}^{1,2}$, as the temperature dropped below $T\approx 0.5J$. Hence spins in different layers moved toward a state of orthogonal order. A nonzero staggered magnetization was observed in each layer. Plots of the interlayer collinear and perpendicular spin-spin correlations for $J/J_{\perp}=0.15,\ 0.25,\ 5.0$ are provided in Fig. 4.

In the ground state, the energy and local spin-spin correlation functions have simple analytic forms. In the (π,π) region of the phase diagram up to $J/J_{\perp}=0.25$, the energy is independent of the intralayer coupling, $E_o(\pi,\pi)=-J_{\perp}$, and the collinear correlations are fixed at 1. In the uniformly twisted phase, (π,q), the energy and interlayer spin-spin correlation are described by $E_o(\pi,q)=-2J-J_{\perp}^2/8J$ and $C_{\parallel}^{\alpha,\beta}=\cos^2 q=J_{\perp}^2/16J^2$. The intralayer spin-spin correlation along the direction of frustration also depends on J and $J_{\perp}$ according to the relation $C_{\parallel}^{\alpha,\alpha}(y)=\cos^2 2q=(J_{\perp}^2/8J^2-1)^2$; the intralayer correlation along $\hat{x}$ is equal to unity. Equations for the perpendicular correlations can be obtained from the identity $C_{\parallel}+C_{\perp}=1$.

Additional insight is obtained by fixing the temperature and sweeping the interaction strength. Runs at $\beta=5,10,\ 20$ were performed and the data for the energy, $C_{\parallel}^{1,2}$, and $C_{\parallel}^{1,1}$ exhibited improved agreement with the $T=0$ analytic forms with increasing inverse temperature. Comparisons for the inter- and intralayer correlations are shown in Fig. 5. We underscore that an orthogonally ordered state is predicted for small interlayer coupling.

These finite-temperature results lend important insight into the temperature at which significant local interlayer order occurs. In particular, we see that local orthogonal interlayer order occurs below $T\approx 0.5J$ when one is in the spin canted region of the phase diagram, which was observed for runs with $J_{\perp}/J=0.2$ and $J_{\perp}/J=1.0$ (data not shown). We also see that the onset of this uniformly canted phase occurs at the predicted ground-state value of $J/J_{\perp}=0.25$ when $T\leqslant 0.25$.

We now consider the temperature dependence of diagonal lattice in the three phases of interest. The run parameters for the zigzag lattice were used with the substitution of periodic for open boundary conditions. We set the intralayer interaction strength to yield the values $J/J_{\perp}=0.15,\ 0.5,\ 1.5,\ 5.0$ and then varied the temperature. Below the transition line, where one is in the (π,π) phase, a collinear state between the layers was found as the temperature dropped below $T\approx J_{\perp}$. Above the transition line, in the $(\pi,0)$ phase, and in the region of experimentally realizable couplings, $J/J_{\perp}=1.5,\ 5.0$, a collinear state was observed at temperatures below $T\approx 0.5J$, in agreement with the zigzag lattice for

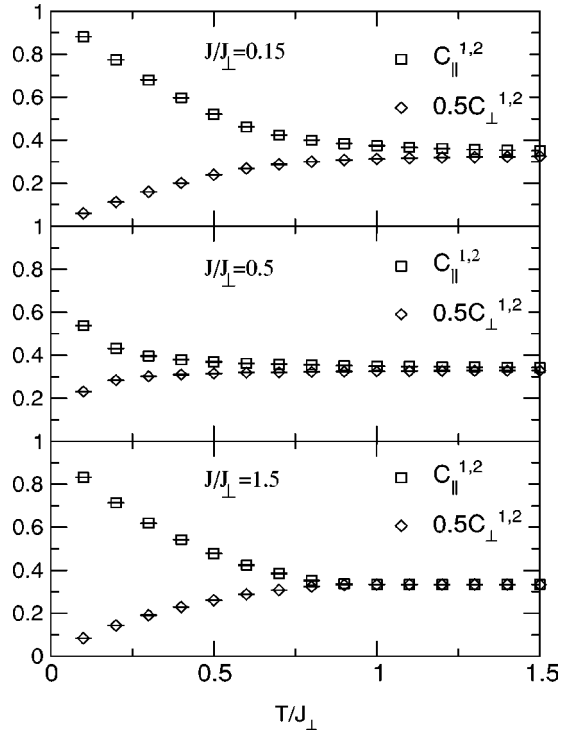

FIG. 6. Temperature dependence of the local interlayer spin-spin correlation functions for the diagonal lattice. $C_{\parallel}^{1,2}$ and $C_{\perp}^{1,2}$ along the $\hat{x}$ and $\hat{y}$ directions are averaged, and $C_{\perp}^{1,2}$ is scaled to give 1/3 in the high-temperature limit. In the three cases shown, one is below, $J/J_{\perp}=0.15$, at, $J/J_{\perp}=0.5$, and above, $J/J_{\perp}=1.5$, the classical transition point of the J_1-J_2 model. A collinear state is demonstrated at low T in all cases.

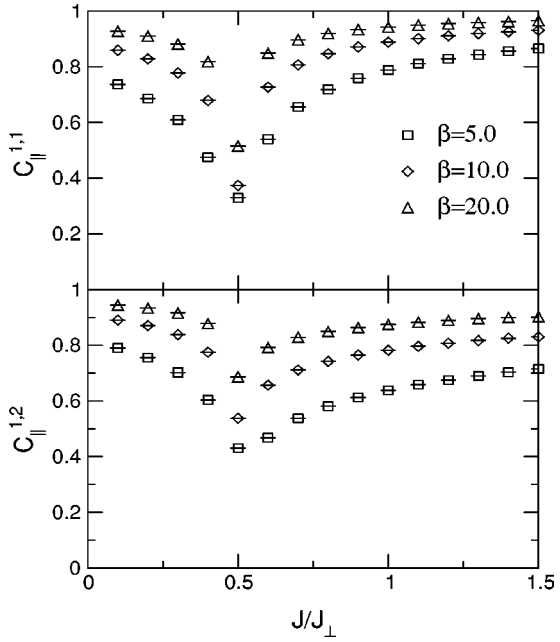

FIG. 7. Interlayer and intralayer correlations as a function of interaction strength for the diagonal lattice. In the bottom panel, a collinear state between spins in different layers is indicated on both sides of the $J/J_{\perp}=0.5$ transition point. In the top panel, spins in the same layer also tend toward a collinear alignment on the two sides of the transition point. The suppression in both correlation functions at $J/J_{\perp}=0.5$ suggests a slight canting of the local moments.

strong J. On the transition line, where a (q,q) phase is expected, a paramagnetic lattice is realized down to $T\approx 0.5J_{\perp}$. At lower temperatures there is a weak separation of the values of $C_{\parallel}^{1,2}$ and $C_{\perp}^{1,2}$, indicating a state canted away from strict collinearity. The Monte Carlo data for $J/J_{\perp}=0.15,\ 0.5,\ 1.5$ are shown in Fig. 6.

In the ground state, the energy takes on simple analytic forms in the regions separated by the line, $J/J_{\perp}=0.50$. Following the description of the planar J_1-J_2 model, the energy below the transition line is given by $E_o(\pi,\pi)=-2J_{\perp}(1-J/J_{\perp})$, whereas above that line the relation is independent of the interlayer coupling, $E_o(\pi,0)=-2J$. On the line the energy is given by $E_o=-2J$, and is highly degenerate. Monte Carlo simulations at fixed inverse temperatures of 5, 10, and 20 capture the essential features of the ground-state phase diagram, these features becoming sharper with increasing β.

In Fig. 7, the collinear spin-spin correlations are enhanced on either side of $J/J_{\perp}=0.5$. The dip at the transition point indicates weak canting between neighboring spins, with the behavior identical along either lattice direction. This suggests the equivalence of the two classically predicted states of (π,q) and (q,π). The simulation also captures the proper energy dependence of the ground state, see Fig. 8. Despite the similar enhancement of $C_{\parallel}^{1,2}$ and $C_{\parallel}^{1,1}$ at low T on both sides of $J/J_{\perp}=0.5$, the two collinear states are not magnetically equivalent. Below $J/J_{\perp}=0.5$ the system consists of two ferromagnetically ordered layers with opposite magnetization; above this line the system organizes into two Néel ordered planes. These features are clearly demonstrated by the magnetization and staggered magnetization data of the identical layers, see Fig. 9. The essential conclusion from our

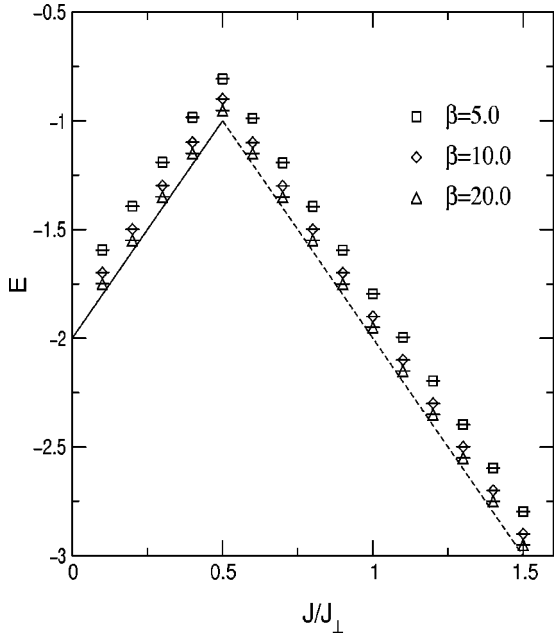

FIG. 8. Average energy as a function of the interaction strength for the diagonal lattice. Monte Carlo data at three inverse temperatures are compared to the $T=0$ analytic solutions $E_o(\pi,\pi)=-2J_{\perp}(1-J/J_{\perp})$ (solid line) and $E_o(\pi,0)=-2J$ (dashed line). We observe convergence to the ground-state results with increasing β.

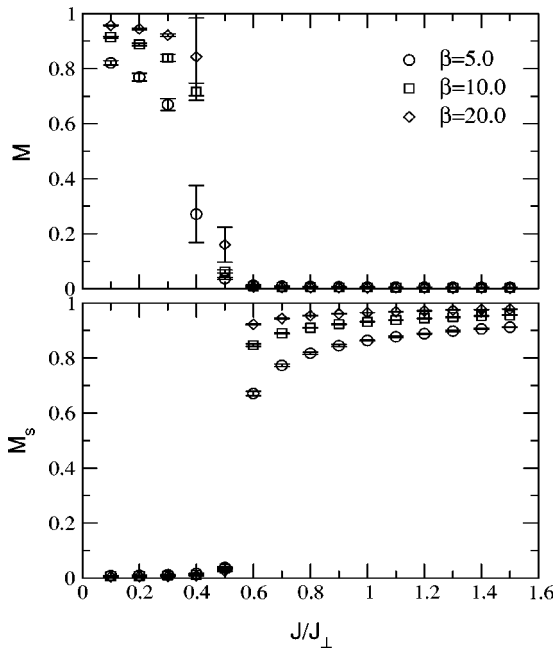

FIG. 9. Magnetization and staggered magnetization as a function of interaction strength for the diagonal lattice. Below $J/J_\perp = 0.5$, we observe a system composed of two ferromagnetic layers with opposite magnetization; above the transition point, the two layers become antiferromagnetically ordered. These two states correspond to the (π,π) and $(\pi,0)$ phases of the planar J_1-J_2 model, respectively.

study of the diagonal lattice is that frustration caused by this geometry does not drive the order in the two layers to lie in perpendicular planes.

III. THE MIXED LAYER PNICTIDE OXIDES

In the preceding section we saw how local interlayer order is established in two simple layered models with geometric frustration. The zigzag lattice gave orthogonal interlayer order at low temperature and weak $J_\perp/J$, but the diagonal lattice exhibited collinear order in this same coupling regime. In this section we develop and investigate a representative model for the mixed layer pnictide oxides; our focus is on the nature of the local interplanar order. As was discussed in Sec. I, these compounds contain square planes of mixed chemical environment which order orthogonally in the ground state, see Fig. 1. The dominant interactions are between nearest neighbors in the same plane, with a weak coupling between sites in adjacent planes. They also possess the interesting features of CuO_2 like planes and a K_2NiF_4 magnetic substructure, both key components to many investigations in metal-oxide materials. The same Monte Carlo techniques used to study the diagonal and zigzag lattices are employed here. We begin with the presentation of our model and then discuss the results from our simulations.

A. The bilayer model

Our bilayer model contains a layer of type Mn(1) and type Mn(2), i.e., the two distinct and inequivalent square planes of the pnictide oxides. One layer is larger by a factor of $\sqrt{2}$ and rotated by $\pi/4$ with respect to the lattice directions of the other layer. Again as in the pnictide oxides, the model has antiferromagnetic nearest-neighbor coupling within each layer and frustration caused by antiferromagnetic interactions between nearest-neighbor spins in different planes. A 2D projection of our bilayer system is given in Fig. 10. We will refer to this model as the mixed layer model. If we let n denote the linear dimension of the smaller lattice, then the Mn(2) layer contains n^2 spins, while the Mn(1) layer contains $n^2/2+n+1$ spins. Note that the interlayer coordination of spins in the two layers is different. A site in the Mn(1) layer has four nearest neighbors of type Mn(2); however, sites in the Mn(2) layer have only two nearest neighbors of type Mn(1). Hence, there are components of both the zigzag and diagonal lattices in this geometry. The model Hamiltonian is similar to Eq. (1), which we explicitly write as

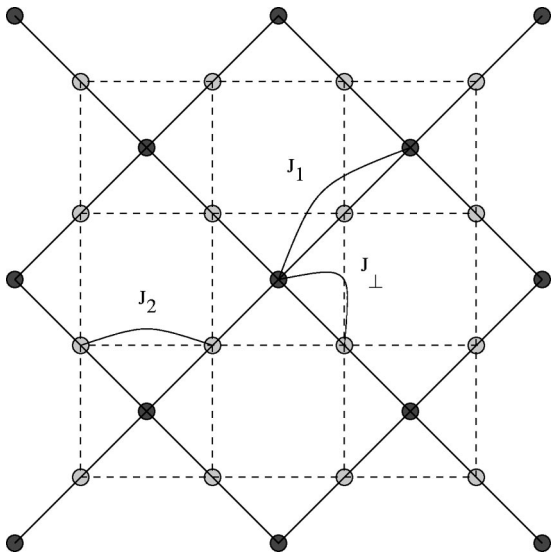

FIG. 10. The mixed layer lattice, a projection of two layers of the experimental geometry onto a plane. Sites in the Mn(1) layer are represented by dark circles, while sites in the Mn(2) layer are represented by light circles. The lattice constant for the Mn(2) plane is set at $a=1$; therefore, the Mn(1) square plane is described by the constant $b=\sqrt{2}$. The intralayer couplings are shown as J_1 and J_2, and the interlayer interaction is indicated by $J_\perp$.

$$H = J_1 \sum_{i,\vec{\delta}_1} \vec{S}_i^{(1)} \cdot \vec{S}_{i+\vec{\delta}_1}^{(1)} + J_2 \sum_{i,\vec{\delta}_2} \vec{S}_i^{(2)} \cdot \vec{S}_{i+\vec{\delta}_2}^{(2)} + J_\perp \sum_{i,\vec{\delta}_\perp} \vec{S}_i^{(\alpha)} \cdot \vec{S}_{i+\vec{\delta}_\perp}^{(\beta)} . \quad (6)$$

The summations of $\vec{\delta}_\mu$ are over nearest neighbors to site i. The exchange interactions for the Mn(1) and Mn(2) layers are J_1 and J_2, respectively, and the interlayer exchange is denoted by $J_\perp$.

B. Monte Carlo results

We have performed simulations of this model for system sizes as large as $n=40$, i.e., 841 sites on the Mn(1) layer and 1600 sites on the Mn(2) layer. Equilibration times ranged from 15 000 to 25 000 sweeps through the lattice followed by as many as 15 000 measurements taken at intervals of 10–25 sweeps. Also, because the mixed layer lattice contains geo-

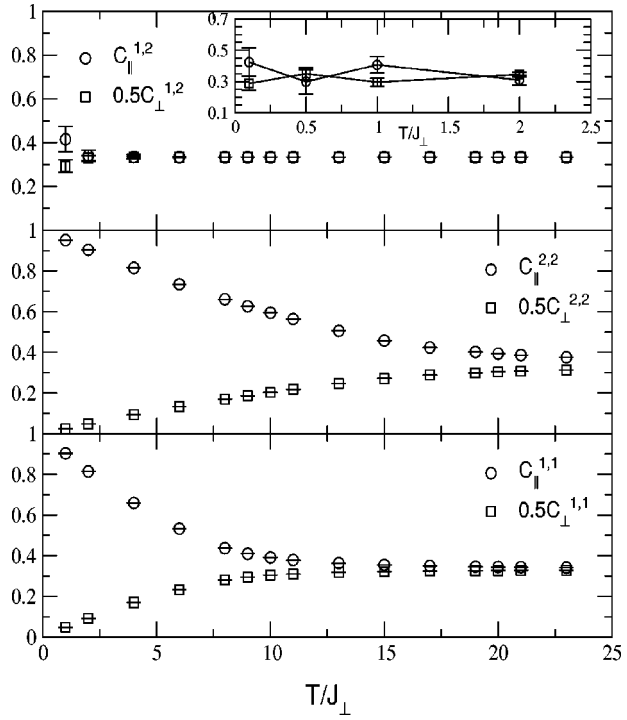

FIG. 11. Temperature dependence of the local interlayer and intralayer spin-spin correlation functions for the mixed layer model, $J_1=1.0$, $J_2=2.0$, $J_\perp=0.1$. In the bottom and middle panels, the collinear and perpendicular correlation functions for the Mn(1) and Mn(2) layers, respectively, are plotted. Neighboring spins within a layer tend toward a collinear alignment when $T\approx J_\alpha$. The interlayer correlations remain at the high-temperature limit, 1/3, for all temperatures, top panel. The inset shows results at low T.

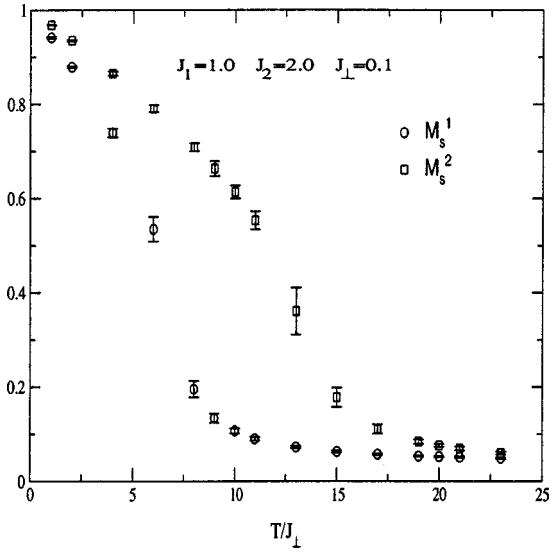

FIG. 12. Temperature dependence of the staggered magnetization for the mixed layer model. The staggered magnetization of the Mn(1) and Mn(2) layers jumps at $T\approx J_1$ and $T\approx J_2$, respectively, which is supported by the enhancement of the local intralayer spin-spin correlations shown Fig. 11.

metric properties that are characteristic to the both the zigzag and diagonal lattices, we wanted to investigate the effect of different boundary conditions on the physics of our model. Hence we simulated the mixed layer model with three different boundary conditions [periodic, open, and periodic with an effective field on the Mn(1) layer] and found no qualitative difference in the results due to the conditions imposed at the boundary. To improve the statistics in the Monte Carlo data, periodic boundary conditions were used in the collection of results presented here. Our discussion begins with Monte Carlo data from fixed interaction and variable temperature runs.

From the experimentally observed ordering temperatures of the two distinct layers, one expects J_2 to be stronger than J_1. Then because of the insulating layer of Sr between the Mn(1) and Mn(2) layers, a $J_\perp$ that is weaker by an order of magnitude is a reasonable expectation. Hence, a mixed layer model with experimentally representative interactions would be roughly described by $J_2=2$, $J_1=1$, and $J_\perp=0.1$. Simulations of this model have been performed, and some results do agree with experiment. The Mn(2) layer orders locally before the Mn(1) layer with the respective ordering temperatures following the trend $T_2\approx J_2$ and $T_1\approx J_1$ as is reasonable. This is clearly demonstrated in the measurements of the intralayer spin-spin correlations, see Fig. 11, where $C_{\parallel}^{\alpha,\alpha}$ breaks from $0.5C_{\perp}^{\alpha,\alpha}$ and the high-temperature limit of 1/3 when the temperature decreases below the exchange energy. Each layer seeks its own Néel state, but as is shown in Fig. 12, the Mn(2) layer is strongly ordered, i.e., $\xi_{\mathrm{Mn}(2)}\approx L_{\mathrm{Mn}(2)}$, by the time the staggered magnetization in the Mn(1) layer begins to rise. The interlayer correlations, $C_{\perp}^{\alpha,\beta}$, remain at the high-temperature limit even below $T=J_\perp$, see top panel and inset in Fig. 11. Hence a transition to a state with significant interlayer order when the temperature is approximately half the intralayer coupling, as observed in the zigzag and diagonal lattices, is not found here. Our calculations, therefore, suggest a system of composed of two independent Néel ordered layers.

If the intralayer couplings are fixed as described above and a sweep in $J_\perp$ is performed, we find, at fixed temperature, that the two layers are ordered antiferromagnetically for all interlayer couplings. Specifically, we observe no variation in the staggered magnetization or the local spin-spin correlations in each layer, see Fig. 13. However, measurements of the interlayer correlations, $C_{\parallel}^{1,2}$, indicate that the two layers are independent for weak $J_\perp$, i.e., $J_\perp<0.25$, the case of weak frustration, but move toward a dominantly collinear arrangement as $J_\perp$ approaches J_1, the case of strong frustration. The fluctuations in $C_{\parallel}^{1,2}$ are significantly greater than in the zigzag or diagonal lattices for $J_\perp<0.6$ and are driven by the competition between collinear and perpendicular ordering tendencies of the geometry. We, therefore, have treated different initial conditions to check our results and observe decoupling of the layers at weak $J_\perp$ independent of whether the initial configuration of the simulation was ordered or random, see Fig. 14. Hence, fluctuations between spins in different layers do not break the continuous symmetry of the ordered state when the frustration is weak but do when it becomes strong, or when $J_\perp\geqslant 0.5$, choosing a collinear state between the layers. As mentioned above, the boundary conditions employed also had no effect on our results. Therefore, in a model with experimentally motivated interaction strengths, frustration alone does not drive the spins in different planes of the mixed layer model to order along perpendicular directions.

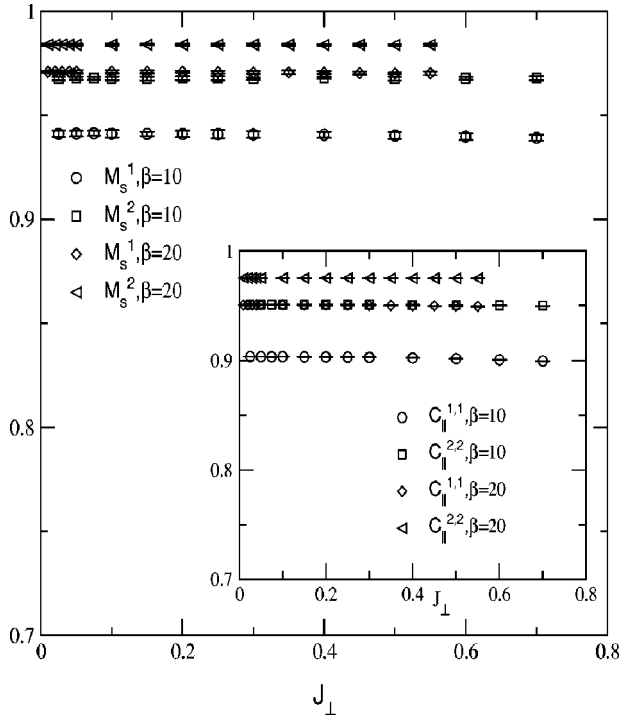

FIG. 13. Magnetic order in the mixed layer model. The local and long-range order within each layer of the model is independent of the interlayer coupling for values representative of the experimental system, $J_1=1.0$ and $J_2=2.0$. M_s^α and $C_\parallel^{\alpha,\alpha}$ are larger in the Mn(2) layer than the Mn(1) layer at fixed temperature.

We verified these qualitative arguments with a few simulations with a larger number of layers. For experimentally motivated interaction strengths, we observed qualitatively the same behavior that was found for the bilayer model. As a function of temperature, the Mn(2) layers order first followed by the Mn(1) layers. The final state is a collinear arrangement of spins on the different layers.

As we move away from experimentally motivated interactions, let us consider several interesting limits to our mixed layer model. At $J_2=0$, the resultant system is a square lattice with three sites per unit cell and a Mn(1) site at the center of the cell. Minimization of the momentum-dependent exchange integral gives $\cos q_x b/2=\cos q_y b/2=-J_\perp/4J$, where b is the lattice constant of the Mn(1) layer. Therefore, a (π,π) state between Mn(1) and Mn(2) spins is expected for $J/J_\perp\leqslant 0.25$, while a uniformly canted state, (q,q), is predicted for $J_1/J_\perp>0.25$. In the limit of weak $J_\perp$, an antiferromagnetic Mn(1) lattice is realized with the Mn(2) sites randomly oriented in a plane perpendicular to the staggered magnetization. Monte Carlo runs at fixed temperature and $J_\perp=1.0$ show a transition to a uniformly twisted state at $J_1\approx 0.25$. In Fig. 15, the interlayer spin-spin correlation function exhibits the same sort of behavior that was observed for the zigzag lattice in Fig. 5. In agreement with the $T=0$ solution, the Mn(1) and Mn(2) lattices have nonzero magnetization below $J_1=0.55$, and in the limit of strong J_1, i.e., $J_1>1.0$, the Mn(1) lattice has a net staggered magnetization. Another interesting limit is obtained when one considers $J_2=J_\perp=1.0$. At $J_1=0$, one has a square lattice with alternating squares centered by isolated Mn(1) spins. The ground state is determined from the solution to $2\cos q_x/2+\cos q_y/2=0$, which yields a Néel ordered Mn(2) lattice with the Mn(1) spins aligned perpendicular to the local Mn(2) environment. There is no long-range order within the Mn(1) plane. The effect of finite J_1 was studied by Monte Carlo,

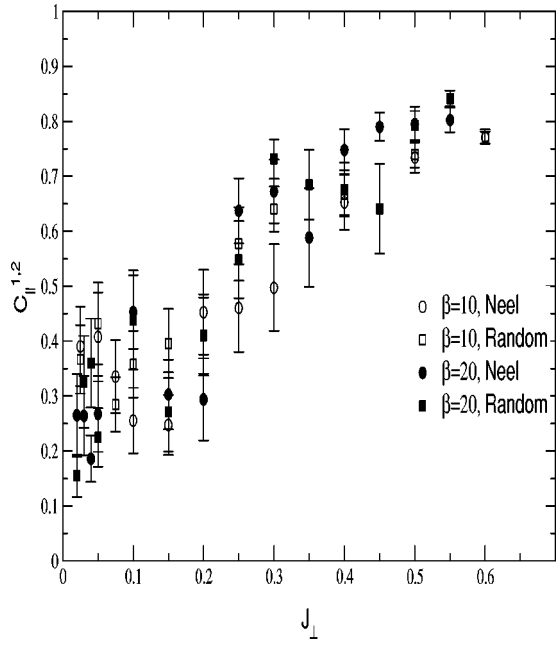

FIG. 14. Interlayer spin-spin correlations as a function of $J_\perp$ with $J_1=1.0$ and $J_2=2.0$. The simulation was initialized in either a random or Néel state. For $J_\perp<0.25$, $C_\parallel^{1,2}$ remains near the paramagnetic limit of 1/3. A tendency toward larger values and thus a more collinear state between the layers occurs for $J_\perp>0.25$. The transition is more abrupt at lower temperatures.

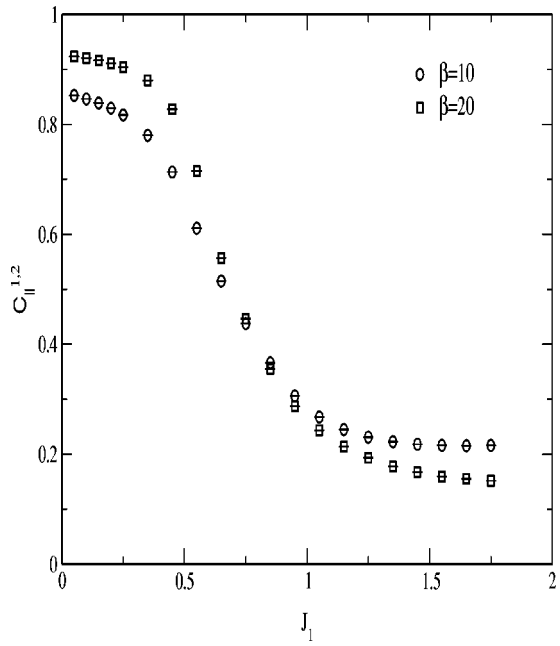

FIG. 15. Interlayer spin-spin correlations in the limit $J_2=0$ and $J_\perp=1.0$. The enhanced values of $C_\parallel^{1,2}$ at weak J_1 indicate a system with local collinear order between the layers. A transition to a uniformly rotated phase at $J_1>0.25$ is marked by a suppression in the interlayer correlations. The behavior here is reminiscent of the situation observed in the zigzag lattice, refer to Fig. 5.

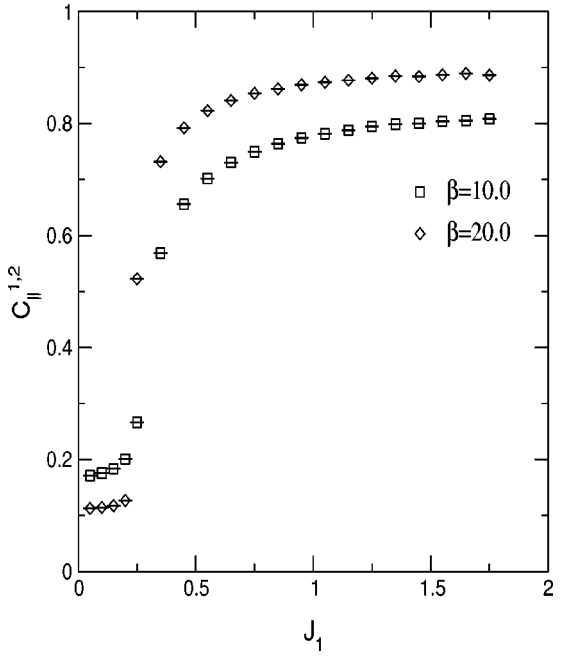

FIG. 16. Interlayer spin-spin correlations of the mixed layer model with $J_2=J_\perp=1.0$. For $J_1\leqslant 0.25$, we observe a trend towards local perpendicular order between the two layers with increasing β. A sharp transition to a local collinear state occurs when the Mn(1) sites are more strongly coupled.

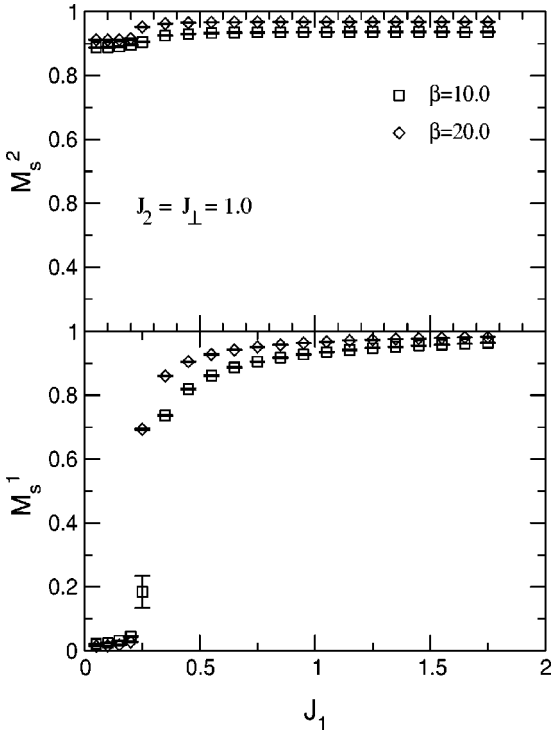

FIG. 17. Staggered magnetization of the mixed layer model with $J_2=J_\perp=1.0$. Our simulations detect a sharp transition in the Mn(1) layer at $J_1>0.25$ from a paramagnet to an antiferromagnet, bottom panel. The Mn(2) layer is antiferromagnetically ordered at all values of J_1, top panel.

and our results support the $T=0$ picture. In particular, we see a trend toward local orthogonal order between the Mn(1) and Mn(2) layers at weak J_1 and low temperatures. We also find that the Mn(2) layer is antiferromagnetically ordered while the Mn(1) layer is paramagnetic. Hence, the orthogonal alignment between moments in different layers is strictly a local phenomena. A transition to a collinear state and Néel order in both planes occurs for $J_1>0.25$. Figures 16 and 17 show the Monte Carlo data for $C_{\|}^{1,2}$ and M_s.

IV. CONCLUSIONS

We have found that frustration caused by lattice mismatch as planes are stacked can lead a layered system to order along orthogonal directions. This perpendicular state is sensitive to the geometric structure and strength of the interactions. Frustration caused by lattice offset along a single direction yields a uniformly twisted state, for $J/J_\perp>0.25$, that becomes orthogonal in the limit of weak $J_\perp$, the coupling responsible for frustration. The temperature dependence of this transition was observed to be $T\approx 0.5J$. The diagonal lattice also exhibited interlayer order at low temperatures, but it was always to a collinear state between the layers. In a mixed layer model appropriate to the pnictide oxides, a local orthogonal state between the layers can be obtained, but its existence is sensitive to the strength of the interactions. Specifically, when $J_2=0$ or $J_2=J_\perp$ a perpendicular state is found for $J_\perp/J_1\rightarrow 0$ or $J_\perp/J_1>4$, respectively. Therefore, simple arguments suggesting ''cancellation'' of interactions due to frustration lead to the absence of order are clearly unfounded.

Although these cases are interesting, they do not represent the experimental system, where $J_\perp$ is expected to be at least an order of magnitude weaker than either of the intralayer interactions. With a model using experimentally reasonable couplings, we observed two independent Néel ordered planes in the case of weak frustration that seek a collinear arrangement as $J_\perp\rightarrow J_1$, or as frustration increases. If viewed as a situation of order from disorder, then the preference for a collinear state is in agreement with the work of Henley.[11]

We emphasize again that even though the crystal structure of the pnictide oxides is three dimensional, the important interactions describe a 2D magnet. The experimental results unambiguously show that order within the planes is established first. It is only as a consequence of these ordered layers that weak three-dimensional order is observed. The effect of ordered planes on the 3D magnetic behavior of layered antiferromagnets has been considered before, both theoretically and experimentally, in the case of K_2NiF_4.[14,8,25] We believe that a better understanding of the various phases of the pnictide oxides would result if a relatively clean crystal could be synthesized and studied.

We conclude that frustration caused by nearest neighbor-interactions, both intra- and interlayer, in the mixed layer pnictide oxides is not sufficient to explain the long-range orthogonal order that is observed experimentally. Thus, in these systems it is likely that other terms in the Hamiltonian, e.g., local anisotropies, are required to explain the magnetic behavior.

ACKNOWLEDGMENTS

We acknowledge the generous support of Campus-Laboratory Collaboration of the University of California, the Materials Research Institute at Lawrence Livermore National

Laboratory, and the Student-Employee Graduate Research program at Lawrence Livermore National Laboratory. We thank Rajiv Singh at the University of California, Davis, Carey Huscroft at the University of Cincinnati, and Dave Feldman at the College of the Atlantic for many useful discussions. We also thank D.P. Landau at the Center for Simulational Physics at the University of Georgia, Athens for helpful suggestions. Work at Lawrence Livermore National Laboratory performed under the auspices of the U.S. Department of Energy under Contract No. W-7405-ENG-48.

[1] D.C. Mattis, in *The Theory of Magnetism II, Thermodynamics and Statistical Mechanics*, edited by P. Fulde (Springer-Verlag, Berlin, 1985); A. Auerbach, *Interacting Electrons and Quantum Magnetism*, edited by J.L. Birman, H. Faissner, and J.W. Lynn (Springer-Verlag, New York, 1994); F. Gebhard, *The Mott Metal-Insulator Transition*, edited by G. Höhler (Springer-Verlag, Berlin, 1997).

[2] K. Binder and A.P. Young, Rev. Mod. Phys. **58**, 801 (1986).

[3] *Spin Glasses and Random Fields*, edited by A.P. Young (World Scientific, River Edge, NJ, 1998).

[4] M.L. Plumer, A. Caillé, and H.T. Diep, in *Magnetic Systems with Competing Interactions (Frustrated Spin Systems)*, edited by H.T. Diep (World Scientific, Singapore, 1994).

[5] H.T. Diep, Europhys. Lett. **7**, 725 (1988); H.T. Diep, Phys. Rev. B **39**, 397 (1989).

[6] H. Kawamura, J. Phys. Soc. Jpn. **54**, 3220 (1985); Phys. Rev. B **38**, 4916 (1988).

[7] S.L. Brock, N.P. Raju, J.E. Greedan, and S.M. Kauzlarich, J. Alloys Compd. **237**, 9 (1996); S.L. Brock and S.M. Kauzlarich, *ibid.* **241**, 82 (1996); S.L. Brock and S.M. Kauzlarich, CHEMTECH **25**, 18 (1995).

[8] R.J. Birgeneau, H.J. Guggenheim, and G. Shirane, Phys. Rev. Lett. **22**, 720 (1969).

[9] J. Leciejewicz, S. Siek, and A. Szytula, J. Magn. Magn. Mater. **40**, 265 (1984).

[10] C.C. Torardi, W.M. Reiff, K. Lázár, J.H. Zhang, and D.E. Cox, J. Solid State Chem. **66**, 105 (1987).

[11] C. Henley, Phys. Rev. Lett. **62**, 2056 (1989).

[12] A. Moreo, E. Dagotto, T. Jolicoeur, and J. Riera, Phys. Rev. B **42**, 6283 (1990).

[13] N.D. Mermin and H. Wagner, Phys. Rev. Lett. **17**, 1133 (1966).

[14] M.E. Lines, Phys. Rev. **164**, 736 (1967); J. Phys. Chem. Solids **31**, 101 (1970).

[15] A.T. Nientiedt, W. Jeitschko, P.G. Pollmeier, and M. Brylak, Z. Naturforsch., B: Chem. Sci. **52B**, 560 (1997).

[16] T. Ozawa, M.M. Olmstead, S.L. Brock, S.M. Kauzlarich, and D.M. Young, Chem. Mater. **10**, 392 (1998).

[17] Y. Park, D.C. DeGroot, J.L. Schindler, C.R. Kannewurf, and M.G. Kanatzidis, Chem. Mater. **5**, 8 (1993).

[18] R.J. Cava, H.W. Zandbergen, J.J. Krajewski, T. Siegrist, H.Y. Hwang, and B. Batlogg, J. Solid State Chem. **129**, 250 (1997).

[19] D. Kaczorowski, J.H. Albering, H. Nöel, and W. Jeitschko, J. Alloys Compd. **216**, 117 (1994); R. Pöttgen, B. Chevalier, P. Gravereau, B. Darriet, W. Jeitschko, and J. Etourneau, J. Solid State Chem. **115**, 247 (1995); J.H. Albering and W. Jeitschko, Z. Naturforsch., B: Chem. Sci. **51B**, 257 (1996).

[20] C.K. Majumdar and D.K. Ghosh, J. Math. Phys. **10**, 1399 (1969).

[21] S.R. White and I. Affleck, Phys. Rev. B **54**, 9862 (1996).

[22] E. Dagotto and A. Moreo, Phys. Rev. Lett. **63**, 2148 (1989).

[23] M.P. Gelfand, R.R.P. Singh, and D.A. Huse, Phys. Rev. B **40**, 10 801 (1989).

[24] N. Metropolis, A.W. Rosenbluth, M.N. Rosenbluth, A.H. Teller, and E. Teller, J. Chem. Phys. **21**, 1087 (1953).

[25] R.J. Birgeneau, H.J. Guggenheim, and G. Shirane, Phys. Rev. B **1**, 2211 (1970); **8**, 304 (1973).